

Exploration of High Harmonic Fast Wave Heating on the National Spherical Torus

Experiment

J. R. Wilson,^{1,†} R.E. Bell,¹ S. Bernabei,¹ M. Bitter,¹ P. Bonoli,² D. Gates,¹ J. Hosea,¹ B. LeBlanc,¹ T.K. Mau,³ S. Medley,¹ J. Menard,¹ D. Mueller,¹ M. Ono,¹ C. K. Phillips,¹ R. I. Pinsky,⁴ R. Raman,⁵ A. Rosenberg,¹ P. Ryan,⁶ S. Sabbagh,⁷ D. Stutman,⁸ D. Swain,⁶ Y. Takase,⁹ J. Wilgen,⁶ and the NSTX Team

Princeton Plasma Physics Laboratory, Princeton University, Princeton, NJ 08543

Massachusetts Institute of Technology, Cambridge MA 02139

University of California, San Diego, San Diego CA

General Atomics, San Diego CA 92186

University of Washington, Seattle WA 98105

Oak Ridge National Laboratory, Oak Ridge TN 37830

Dept. of Applied Physics, Columbia University, New York NY 10027

Johns Hopkins University, Baltimore MD

University of Tokyo, Tokyo, Japan

High Harmonic Fast Wave (HHFW) Heating has been proposed as a particularly attractive means for plasma heating and current drive in the high beta plasmas that are achievable in spherical torus (ST) plasmas. The National Spherical Torus Experiment (NSTX) [Ono, *et al.*] is such a device. An rf heating system has been installed on NSTX to explore the physics of HHFW heating, current drive via rf waves and for use as a tool to demonstrate the attractiveness of the ST concept as a fusion device. To date, experiments have demonstrated many of the theoretical predictions for HHFW. In particular, strong wave absorption on electrons over a wide range plasma parameters and wave parallel phase velocities, wave acceleration of energetic ions and indications of current drive for directed wave spectra. In addition HHFW heating has been used to explore the energy transport properties of NSTX plasmas, to create H-mode discharges with large fraction of bootstrap current and to control the plasma current profile during the early stages of the discharge.

I. INTRODUCTION

The mission of the National Spherical Torus Experiment¹ (NSTX) includes the demonstration of non-inductive current generation and sustainment required for an attractive ST fusion device as well as exploration of the plasma physics of high β , collisionless, toroidal plasmas at low aspect ratio. In order to achieve these goals auxiliary heating and current drive techniques are required to supplement the modest ohmic heating capabilities inherent in the ST concept. A high β plasma intrinsically has a high value of the plasma dielectric constant, $\epsilon = (\omega_{pe}/\omega_{ce})^2 = \epsilon_0 (c/v_{th})^2$, where $\omega_{pe} = (4\pi n_e^2/m_e)^{0.5}$ is the electron plasma frequency, $\omega_{ce} = eB/m_e c$ is the electron cyclotron frequency and v_{th} is the electron thermal velocity. For NSTX this value is ≥ 50 . Conventional lower hybrid and electron cyclotron waves will not propagate at such large values of β . While conventional fast wave Ion Cyclotron Range of Frequency (ICRF) heating is possible at high β , High Harmonic Fast Wave (HHFW) heating² offered two attractive features for application on NSTX: First, it is attractive from the physics standpoint due to the large single pass damping decrement in to the electrons and weak ion damping; Second, it allowed the re-utilization of the rf equipment used for conventional ICRF experiments on the Tokamak Fusion Test Reactor (TFTR). To date experiments have validated the main ideas behind HHFW physics. Electron heating has been observed under a wide variety of conditions. Interaction of the rf wave with energetic ions has been observed while thermal ion heating has been minimal as predicted for the parameters so far achieved on NSTX. Evidence of current drive with directed spectra has been obtained from magnetic measurements and application of HHFW power has allowed for an exploration of ST

physics: H-modes, internal transport barriers (ITB) and the underlying energy transport mechanisms. In the main body of the paper we will give a brief overview of the basic theory behind HHFW physics, a description of the NSTX HHFW system and a summary of experimental results in NSTX.

II. THEORY OF HHFW HEATING

The basic theory for HHFW heating of high β plasmas was elucidated by Ono². The wave used for HHFW remains the fast magnetosonic wave used for conventional ICRF. Because of the large harmonic number (in these NSTX experiments, $9 < n/n_i < 13$) the thermal ion cyclotron damping can be quite weak while the electron damping can be strong.

When $\beta \gg \beta_i$ and β_e is substantial the damping of the wave on electrons is increased for two reasons. First, the Landau damping term, from the zz component of the dielectric tensor, no longer cancels against the cross, yz component, term. Second, the ratio of the imaginary part of the wave number to the real part, which is proportional to $\beta\beta/\beta_i$, increases for both larger values of beta and harmonic number. These two effects lead to a significant increase in the per pass damping of HHFW waves so that unlike ICRF direct electron damping rates of $<15\%$ per pass it is not unusual to expect 100% damping in a single pass through the NSTX plasma. In fact, since the damping is so strong at high β , the wave power can be significantly damped before it reaches the center of the plasma. This feature, in contrast to the always centrally peaked direct electron damping in conventional ICRF, allows for the

possibilities of off-axis current drive and radial deposition control via control of the launched wave spectrum.

Ion damping is weak at low ion temperature since cyclotron absorption for small $k_{\text{perp}}\rho_i$ is proportional to ρ_i^{n-1} where $\rho_i = (k_{\text{perp}}\rho_i)^2/2$ and n is the cyclotron harmonic number. In NSTX damping on energetic ions from neutral beam injection (NBI) can be important since $\rho_i > 1$ and the absorption approaches the un-magnetized plasma limit from perpendicular ion Landau damping and is proportional to $T_{\text{hot}}^{-3/2}$.

III. DESCRIPTION OF THE NSTX HFW SYSTEM

The NSTX HFW system features a twelve-element antenna, six rf transmitters, a transmission system and a power dividing and decoupling network³.

- A. The antenna consists of twelve identical modules each comprised of a solid copper radiating element fed at one end and grounded at the other to the antenna back plane, a 50% transparent Faraday shield and a protective surround. The antenna module is shaped to poloidally conform to the plasma. The Faraday screen is composed of individual molybdenum U-shaped pieces, which are mechanically attached to the slotted side-walls of the antenna box. The antenna surround is composed of boron nitride plates mechanically mounted into holders. The surround provides an insulating surface for plasma

scrape-off that should minimize rf driven sheath formation. Each antenna element has its own coaxial rf vacuum feedthrough,

B. The six rf transmitters are tuned to a fixed frequency of 30 MHz and are rated for NSTX purposes at 1 MW delivered power for 5 s. The amplitude and phase of each amplifier are individual controllable. The phase velocity of the launched rf wave is controlled by varying the phase relationship between the transmitters. A sample of the rf voltage is taken near the vacuum feedthrough and used in a digital phase feedback system to provide this phase control. The phase can be varied during the shot to reproduce a pre-programmed waveform.

C. Since there are twelve antenna elements and only six transmitters the rf power must be divided to feed the antenna. In addition, the degree of phase control required to achieve the desired antenna spectra requires cancellation of the mutual inductance between the antenna elements. To accomplish both of these tasks a network of precision tuned transmission lines and lumped reactive elements is placed between the transmitters and the antenna. A schematic of this arrangement is shown in figure 1. This network divides the power from each transmitter into two lines and applies then to the i^{th} and $i^{\text{th}}+6$ ($1 < i < 6$) antenna element. Since this is done by means of resonant lengths of transmission line the phase between these pairs of antenna elements is a fixed 180° . Shunt transmission line connections (elements D1-D6 in fig. 1) between each pair of transmitters cross couple power with the precise amplitude and phase relationship required to cancel the nearest neighbor mutual inductance

of the antenna array. This cancellation is sufficient to allow the desired external phase control during plasma operation. A residual next-nearest neighbor mutual remains, which prevents complete phase control during vacuum conditioning. Impedance matching between the transmitters and the antenna decoupling system is accomplished with standard quarter wave transformers and adjustable line stretchers and tuning stubs, all in 9-inch coaxial transmission line.

RESULTS OF NSTX HHFW EXPERIMENTS

The HHFW experiments on NSTX have set out to elucidate the physics of HHFW wave propagation and absorption and to utilize HHFW as a tool for ST physics exploration. The initial experiments concentrated on establishing the absorption characteristics for the wave. NSTX target plasmas having a range of plasma parameters have been investigated: $B_T = 0.3\text{-}0.5$ T, $I_p = 0.3\text{-}0.9$ MA, $\langle n_e \rangle = 0.3 - 3.8 \times 10^{19} \text{ m}^{-3}$, $T_e(0) = 200 - 700$ eV. Both ^4He and D plasmas have been investigated in limiter and divertor configurations. It was quickly observed that electron heating was the dominant effect as predicted by theory. Heating has been observed for a range of launched toroidal wave numbers, $k_{\parallel} = 3\text{-}14 \text{ m}^{-1}$. At $k_{\parallel} = 14 \text{ m}^{-1}$, utilizing waves with the slowest toroidal phase velocity, heating has been observed with target temperatures as low as 200 eV, (fig. 2). As the launched parallel wavelength is increased the rate of central electron temperature increase slows. To check the theoretical prediction that the electron absorption should move off axis as the target plasma electron beta is increased it would

be desirable to have a direct measurement of the power deposition profile. Normally, this would be achieved by modulating the rf power and measuring $T_e(r,t)$ with a fast electron temperature diagnostic such as electron cyclotron emission (ECE) and then performing either break in slope or Fourier analysis of the signals. In an ST ECE cannot be used because of lack of accessibility of the waves from the plasma core to the edge. On NSTX a multi point repetitive Thomson scattering system is used to obtain the electron temperature profile. This system utilizes two independent 33 Hz lasers whose relative timing can be adjusted. An attempt to measure the electron temperature response to a fast change in the rf power level was made by varying the time between laser measurements. It was found that the electron temperature profile was very “stiff” with little immediate response to the removal of power followed by a general relaxation of the temperature profile. This is consistent with theoretical predictions that electron temperature gradient modes determine the electron heat loss. Some indication of off-axis absorption is obtained in shots with higher electron beta that exhibit broader T_e profiles with the rf heating. These discharges show the broadened profiles in the absence of any accompanying MHD that might have broadened the profiles even with peaked power deposition. Global energy confinement in discharges with electron heating is in agreement with predictions from standard L-mode scalings.

Large increases in central electron temperature are obtained in specific cases of HHFW heating; $I_p = 800$ kA deuterium plasmas at moderate density. These discharges are characterized by a central region, $r/a \leq 0.5$, in which the electron transport is much reduced. Peaked temperatures as high as 4 keV are obtained in these discharges with χ_e reduced by as much as a factor of 10 in the core as the barrier develops.

The principal motivation for including the HHFW system on NSTX was the desire to produce non-ohmic current drive to demonstrate the potential of the ST concept as a steady-state plasma device. Current drive with direct electron absorption has been observed on a variety of devices, in particular operation at cyclotron harmonic numbers as high as eight was explored on the D-III-D tokamak⁴. Experiments on NSTX were conducted at harmonic numbers 9-12 where thermal ion absorption should be minimal. In addition electron beta values on NSTX should allow much higher single pass damping values. The low aspect ratio of NSTX, $R/a=1.25$ strongly influences the wave propagation (the waves develop much larger values of k_{\perp} and can fail to propagate all the way to the center of the discharge) and increases the reduction in driven current due to trapped electrons. Experiments have been conducted on NSTX to make a preliminary assessment of the viability of HHFW current drive. In the absence of an MSE diagnostic to measure local changes in the magnetic field the experiments were designed to maximize the expected changes in loop voltage that would arise from driving current. To maximize the expected loop voltage changes and minimize the interference from bootstrap current effects these experiments were conducted at low current, $I_p = 500$ kA and low β , less than 10 percent. Discharges with the rf antenna phased to drive current with, Co, and against, Counter, the pre-existing ohmic current were executed. The observed loop voltage was seen to be very sensitive to the electron density and temperature obtained during the rf pulse. Power levels were adjusted to obtain equal temperatures and gas fueling was adjusted to obtain near equal density profiles, (fig. 3). Under these conditions differences in the loop voltages between co-, $k_{\perp} = +7$ m⁻¹, and counter, $k_{\perp} = -7$ m⁻¹, phased discharges were obtained, (fig. 4). The time evolution of the

differences indicate that as central MHD, sawtooth like behavior, sets in the amount of driven current appears to diminish. If strong central MHD is present before the rf is applied no loop voltage difference is observed. As was observed on D-IIIID less power is needed for counter-phasing than for co-phasing to obtain the same central electron temperature. This difference in required power decreases at lower k_{\perp} . To estimate the current driven in this case we perform a simple circuit calculation that assumes that the discharges have the same resistivity, matching the temperature density and Z_{eff} gives reasonable confidence that this is true, and that takes into account the change in internal inductance. The observed loop voltage difference of 0.22 V corresponds to ~ 180 kA of driven current, 110 kA co and 70 kA counter. Theoretical estimates for these discharges have been made using both the CURRAY⁵ ray tracing code (169 kA co and 79 kA counter) and the TORIC⁶ full wave analysis code (96 kA co and 50 counter). These estimates point out the importance of trapping in determining the efficiency of current drive. With the effects of trapping turned off TORIC predicts nearly 400 kA of current would be driven, (fig. 5). The efficiency of current drive is given in terms of a figure of merit, $\eta_{\text{CD}} = 0.05 \text{ Am}^{-2}/\text{W} \times 10^{19}$, comparable to that observed on previous experiments given the lower electron temperature^{4,7,8}. The normalization for temperature has been given by D-IIIID as $\eta_{\text{CD}} = \eta_{\text{CD}}^* 3.27/T_e(0)$. For NSTX $\eta_{\text{CD}} = 0.15$. The best current drive efficiencies on D-IIIID were higher and parasitic ion absorption was blamed for lower efficiency shots. This should not be the case for these NSTX discharges. Trapping, however, will play a stronger role at the lower aspect ratio of NSTX. In addition, if wave absorption is not single pass, as is the case in these low β discharges, and the edge density is high enough such that the low field side cut-off is in the plasma periphery, loss

of rf power due to waves not reflecting off the low field side cut-off is possible. This effect was invoked to explain some lower efficiency shots on D-IIID. On NSTX the low field side cut-off is always in the plasma periphery and in lower single pass conditions such as those for these particular discharges the wave trajectories touch the low field edge several times before all the power is expected to damp. If the wave is approaching the edge near a material object, e.g. passive plate, or neutral beam armor an rf sheath might form which can dissipate rf power. ■■■

Absorption of the HHFW wave energy by energetic ions presents a parasitic mechanism that can reduce current drive efficiency. In NSTX's most recent campaign, a clear fast ion tail was observed on the neutral particle analyzer (NPA) when HHFW and NBI were active simultaneously. Neutron detector and ion loss probe signals provided further evidence for interaction. This occurred for essentially every shot there was a significant overlap in RF and NBI power traces. Ray-tracing was used to analyze these shots, and found absorption by fast ions to be competitive with electron absorption. Measured neutron rates for similar RF and no-RF shots were also compared with predicted rates, and a significant RF-induced enhancement was found, consistent with the enhanced tail.

For most shots analyzed, the neutral beam injected deuterium into the plasma at $E_b \approx 80$ keV, $P_b \approx 1.6$ MW. Without RF, the energy spectrum observed by the NPA dropped out above ~ 80 keV. With RF, the energy spectrum extended to ~ 140 keV. Furthermore, after RF turnoff with NBI remaining active, the tail decayed to the no-RF spectrum on a time scale comparable to that for decay of a beam-only distribution, as seen in Fig 6.

The ZnS and fission neutron detectors also saw a significant signal enhancement with RF, which also began dropping immediately upon RF turnoff. Sets of similar shots with different B_0 , I_p , E_b , and launched k_{\parallel} were examined. In agreement with modeling, the tail strength and neutron rate at lower B-fields were observed to be less enhanced, likely due to a larger value of \square , which promotes greater off-axis electron absorption where the fast ion population is small. Tail strength also increased with higher beam energy, and a substantial neutron rate enhancement was observed at higher I_p . Though greater ion absorption is predicted with lower k_{\parallel} ^{9,10}, surprisingly little variation in the tail was observed, along with a small neutron enhancement with higher k_{\parallel} . The NPA was also scanned horizontally, and flux of fast particles decreased away from the magnetic axis, while the energy range of the tail remained the same through 40 cm away. In addition to the NPA and neutron detectors, ion loss probes at $R = 163$ cm and 166 cm saw a signal enhancement with RF on in beam shots.

For analysis, the TRANSP transport analysis code was used to calculate fast ion energy and particle density profiles, and this information was used to estimate an effective Maxwellian temperature, T_i , for the fast ion population. This, along with EFIT and Thomson data, was fed into HPRT, a 2-D ray-tracing code¹⁰, which uses the full hot plasma dielectric to compute power deposition profiles along the hot electron/cold ion ray path⁷. Fast ion absorption was calculated to be quite competitive with electron absorption in sustained neutral beam shots, often taking $\sim 40\%$ of the total RF power. These results and profiles matched those of CURRAY, an independently developed ray-tracing code, strikingly well. AORSA¹¹, an all orders full wave code, also found a similar power split using analytic approximations to the above data. Without providing RF input in either

case, TRANSP was also used to calculate the neutron rates for similar RF and no-RF shots. The measured rate matched the prediction well in the no-RF case, and for the RF shot grew to nearly double the predicted rate. It then decayed to approximately the computed rate after RF turnoff.

IV. SUMMARY

Experiments to investigate the physics of HHFW heating and current drive in an ST geometry have been carried out on the NSTX device. As expected from theoretical modeling the rf power is absorbed almost entirely by the electrons for the parameters of the NSTX experiment. Global energy confinement for discharges heated via the electron channel is in reasonable agreement with the predictions of standard tokamak scaling. Under some circumstances improved electron energy confinement is observed and central electron temperatures of 4 keV have been achieved.

In initial experiments with the antenna phased to launch a directed spectrum differences in loop voltage have been observed consistent with plasma current being driven by the wave. The value of current driven, inferred from the magnetic measurements, is ~ 100 kA and is roughly consistent with theoretical estimates. To achieve larger quantities of driven current both higher rf power and higher electron temperatures will be required.

Experiments with combined HHFW and NBI reveal an acceleration of the beam ions by the rf. An ion tail extending, from the 80 keV injection energy out to 140 keV, is observed. This ion absorption which modeling predicts could absorb as much as 50% of

the rf power will lower current drive efficiency. The absorption is predicted and observed to be lower at higher β .

V. ACKNOWLEDGEMENTS

This work supported by United States Department of Energy Contract Numbers DE-AC02-76CH03073 at the Princeton Plasma Physics Laboratory, DE-AC05-96OR22464 at the Oak Ridge National Laboratory, DE-FG02-99ER-54521 at MIT, DE-FG06-90ER54095 at the University of Washington, DE-FG02-89ER53297 at Columbia University and DE-AC03-99ER54463 at General Atomics.

REFERENCES

1. Ono, M. et al., Proceedings 18th IEEE/NPSS Symposium On Fusion Engineering, Albuquerque, 1999, IEEE, Piscataway, NJ (1999) **53**.
2. Ono, M., Physics of Plasmas, **2**, (1995) 4075.
3. Ryan, P.M. et al., Fusion Engineering and Design 56-57, (2001) 569.
4. Petty, C. et al., Plasma Physics and Controlled Fusion, **43** (2001) 1747.
5. Mau, T.K. et al., Radio Frequency Power in Plasmas (Proc. 14th Topical Conference, Oxnard CA, 2001) American Institute of Physics, New York (2001) 170.
6. Brambilla, M., Plasma Physics and Controlled Fusion, **41**, (1999) 1.
7. Rogers, J. et al., Proceedings 16th International conf. On Fusion Energy, Montreal Canada 1996 Vol. 3 317.
8. Majeski, R. et al., Physical Review Letters **76** (1996) 764.
9. Lashmore-Davies, C.N. et al., Physics of Plasmas, **5**, (1998) 2284.
10. Menard, J. et al., Physics of Plasmas, **6**, (1999) 2002
11. Jaeger, E.F., et al., Radio Frequency Power in Plasmas (Proc. 14th Topical Conference, Oxnard CA, 2001) American Institute of Physics, New York (2001) 369.

FIGURE CAPTIONS

Fig. 1 Schematic diagram of the rf distribution system showing the twelve antenna elements, the six rf inputs (T_1 - T_6) and the splitting decoupling network (D1-D6).

Fig. 2 Electron heating on NSTX (a) Time evolution of the electron temperature, plasma current and rf and NBI power. The NBI is in short blips to get the ion temperature via charge exchange recombination spectroscopy. (b) The electron and ion temperature profiles at $t = 0.25$ s.

Fig.3 The time evolution of the electron temperature and density for Co (solid) and Counter (dashed) current drive phasing of the rf.

Fig. 4 Time evolution of the loop voltage for Co and Counter phasing for the same discharges as in figure 3.

Fig. 5 Theoretical driven current profile with and without trapping for the Co current drive shot in figure 3 as predicted by the TORIC wave code. The profile is significantly narrower with trapping effects turned on.

Fig. 6 Neutral particle charge exchange flux as a function of energy showing the decay of the tail above the 80 keV injection energy after the turnoff of rf.

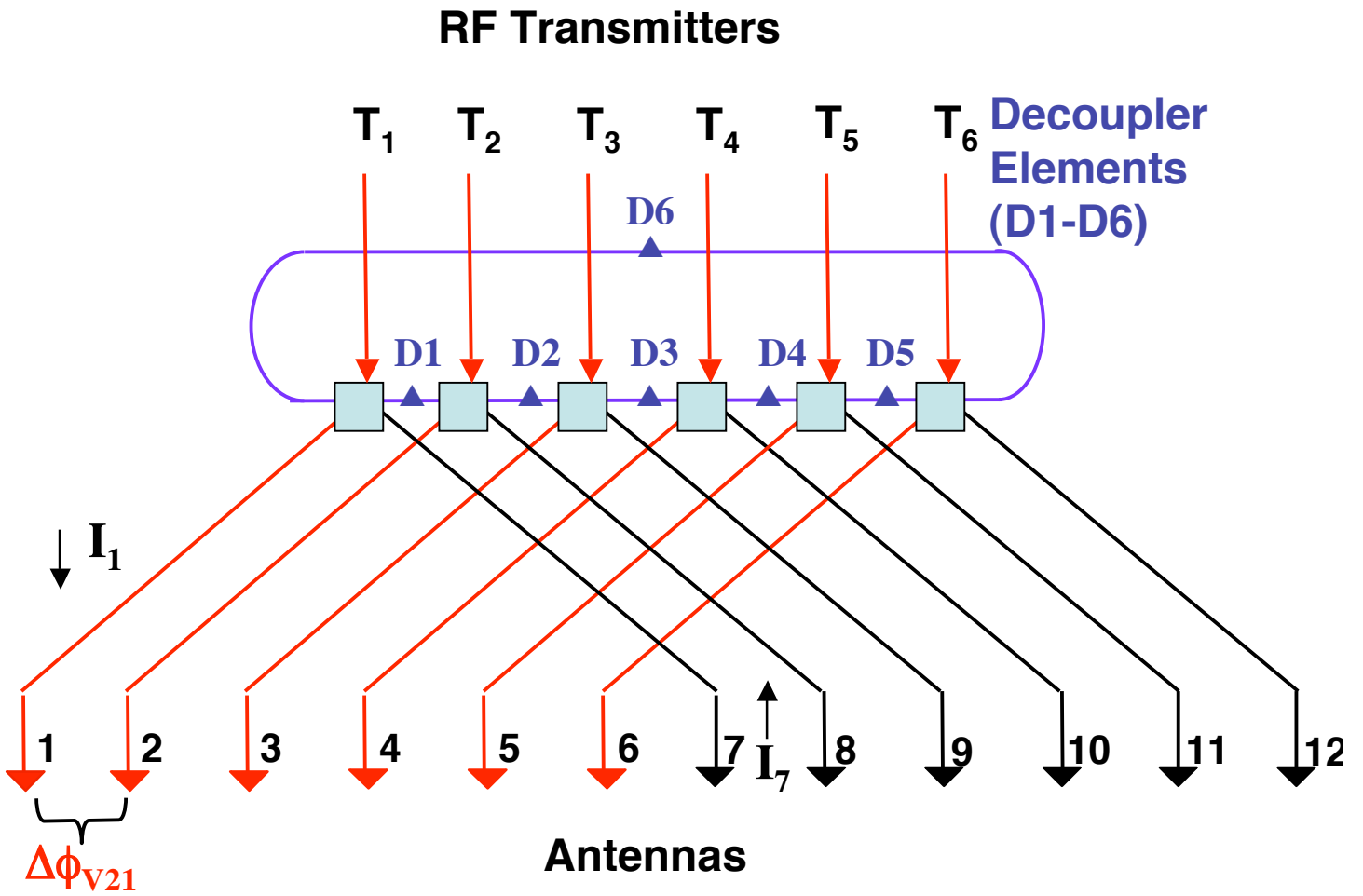


Figure 1

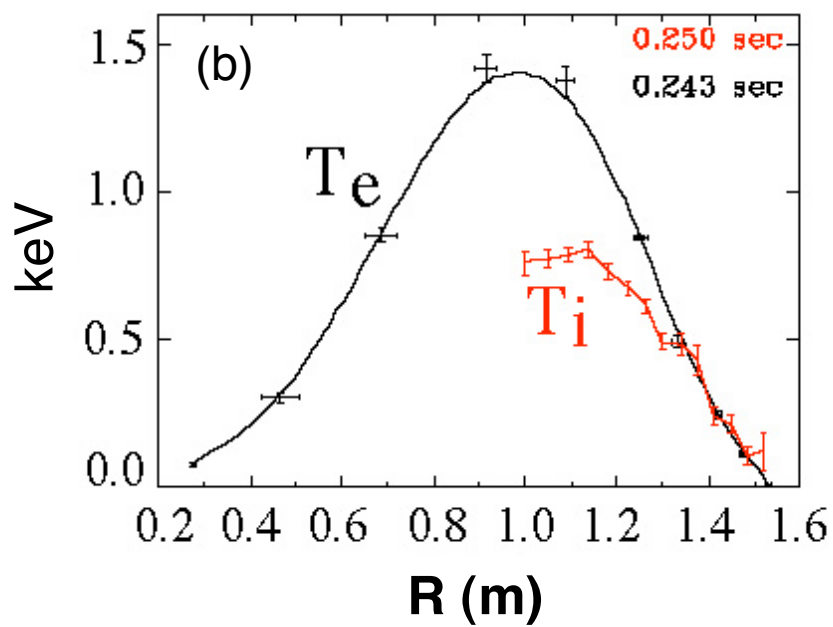
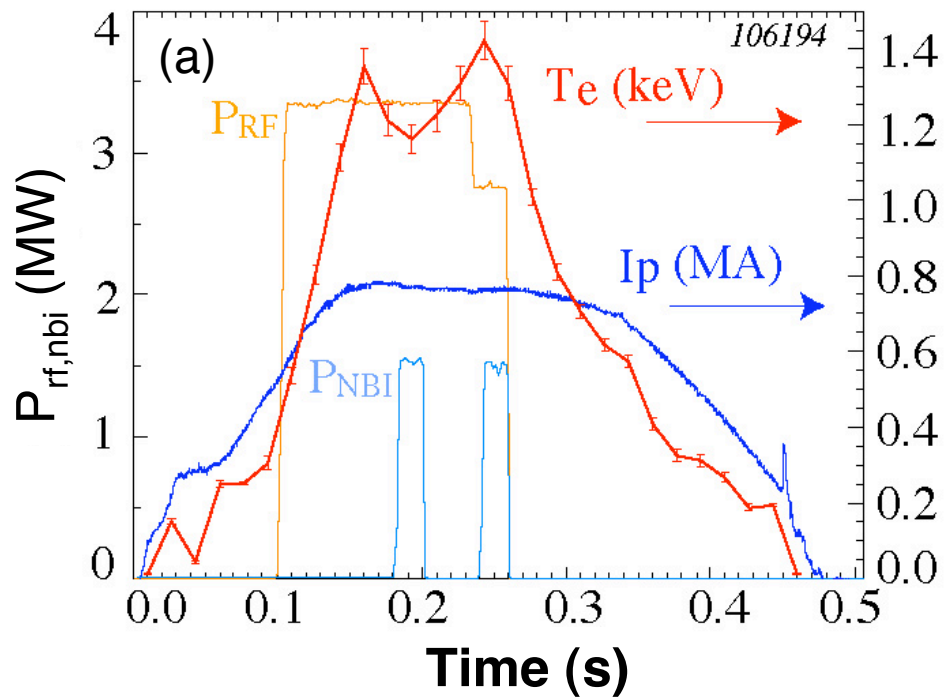


Figure 2

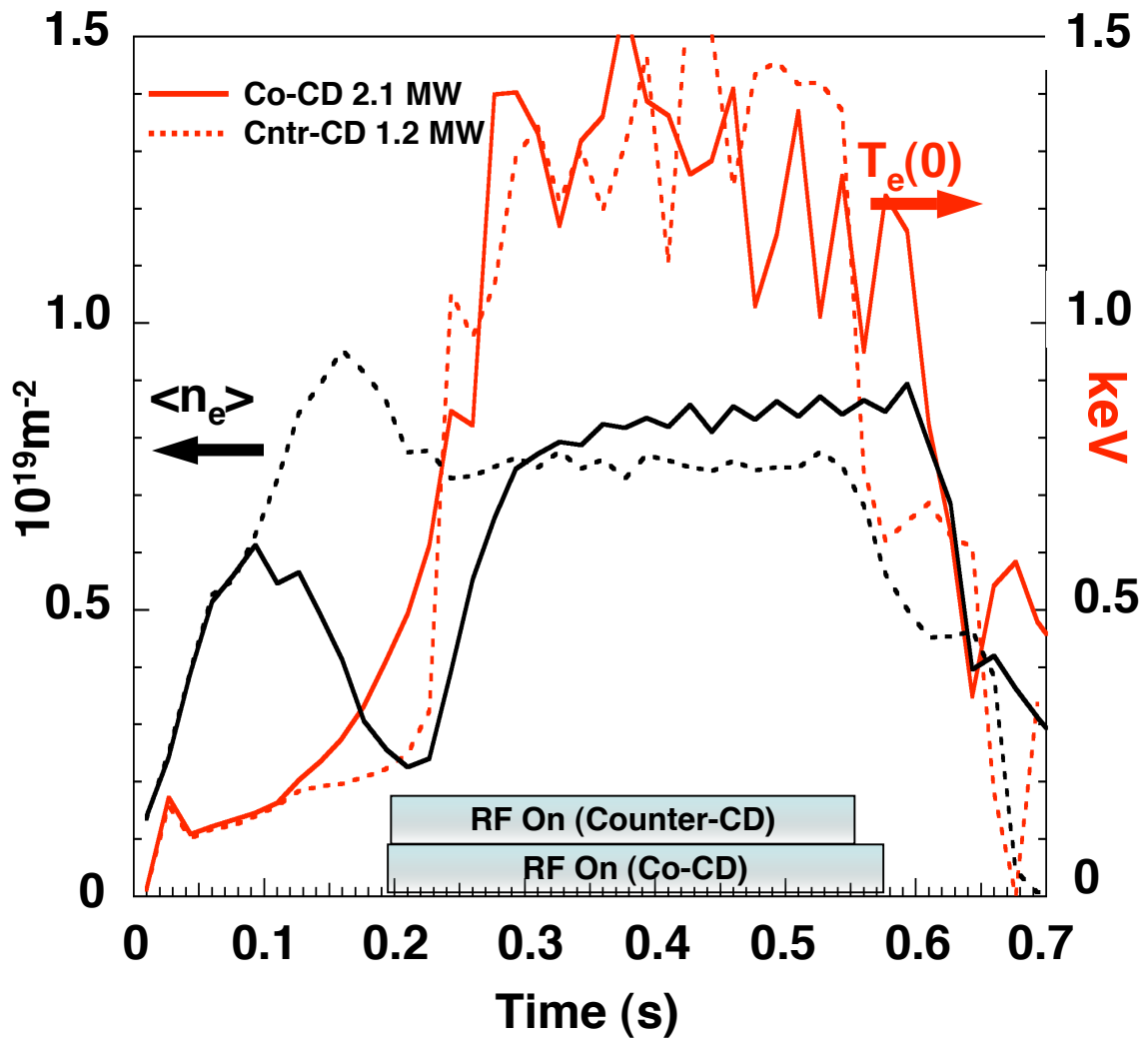


Figure 3

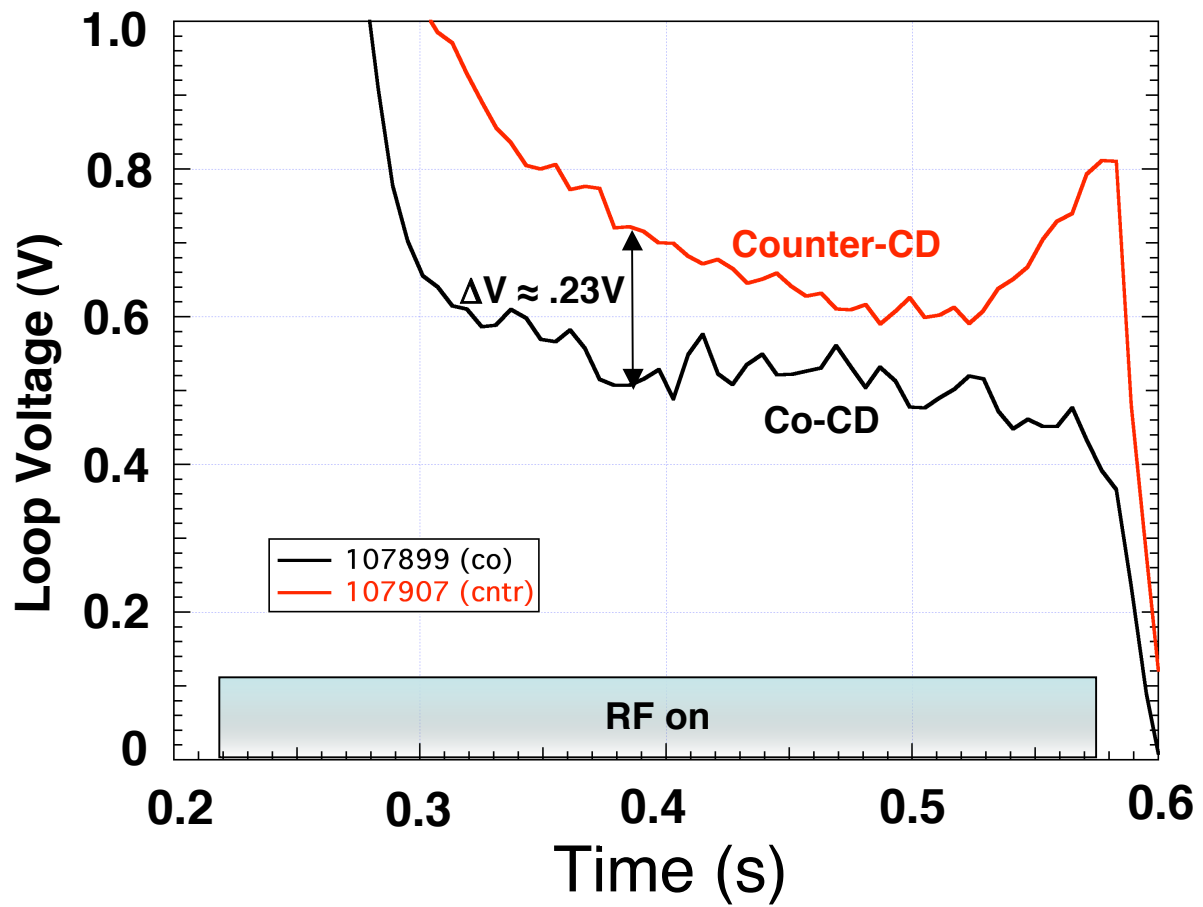


Figure 4

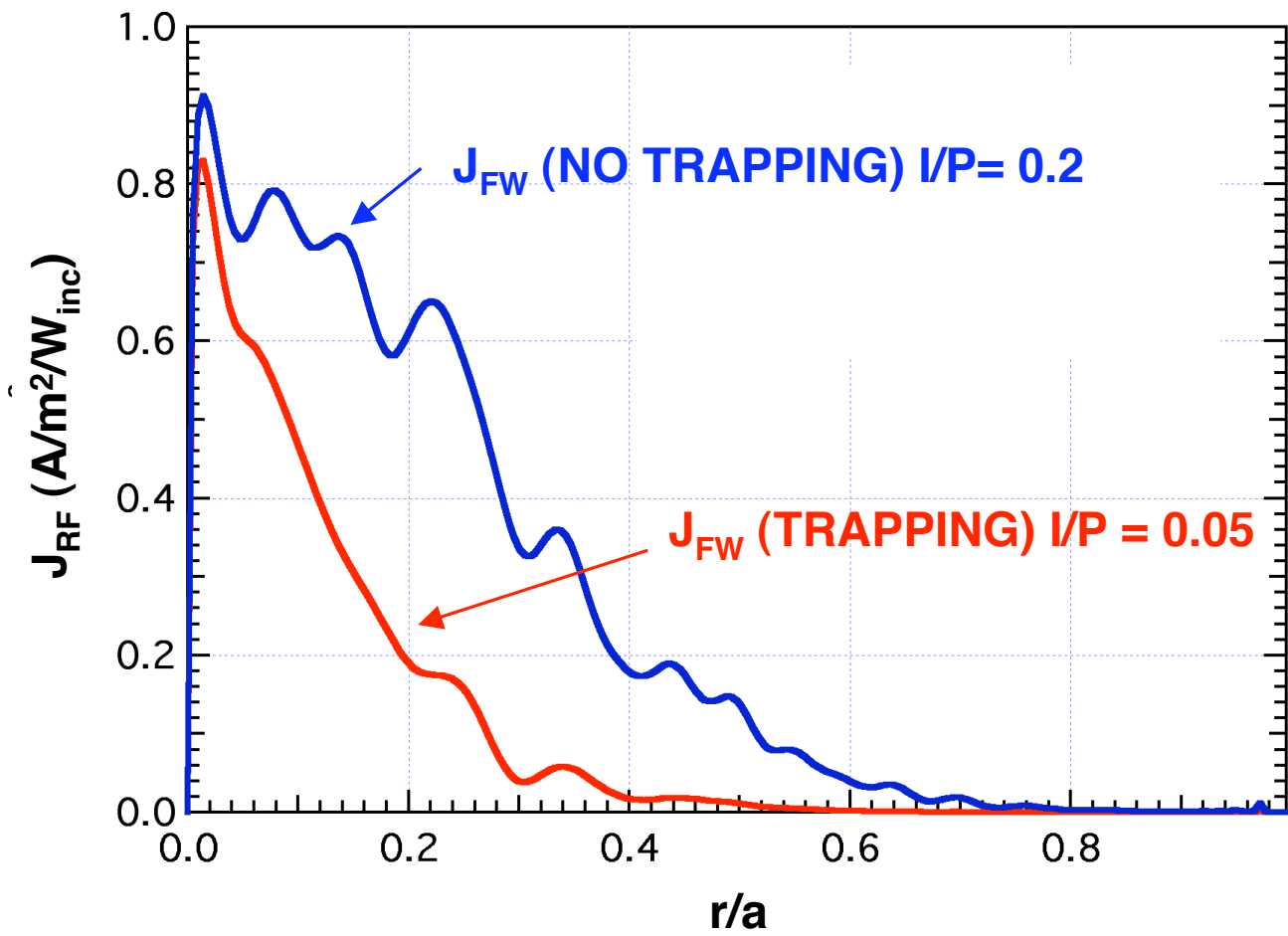


Figure5

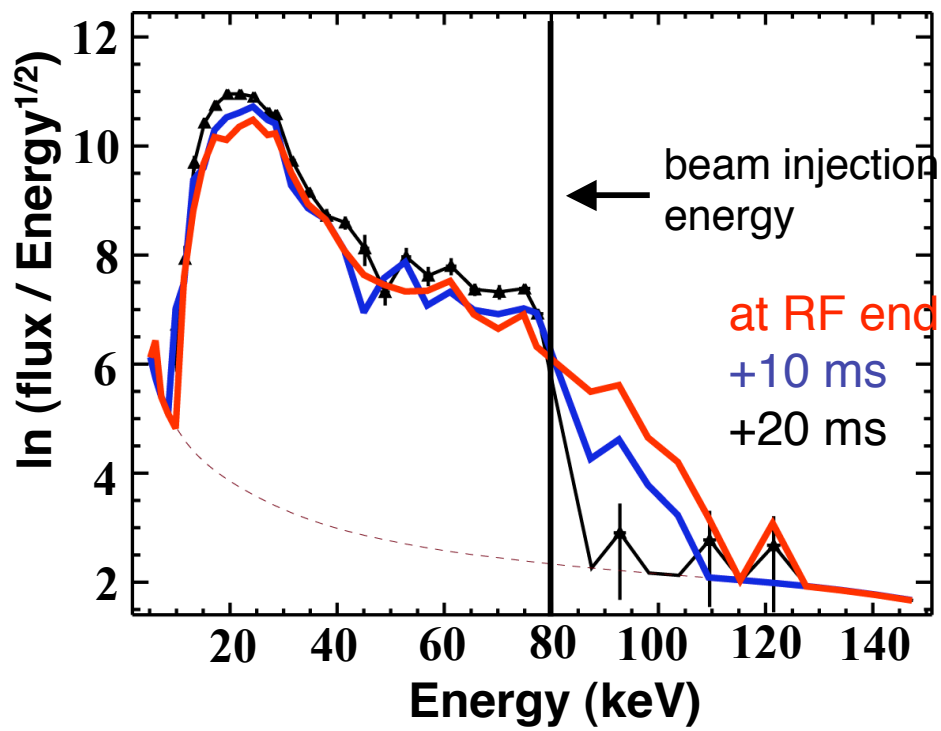


Figure 6